Title

Wintertime atmospheric response to Atlantic multidecadal variability: effect of stratospheric representation and ocean–atmosphere coupling

Journal

Climate Dynamics, 47(3-4)

ISSN

0930-7575

Authors

Peings, Yannick
Magnusdottir, Gudrun

Publication Date

2016-08-01

DOI

10.1007/s00382-015-2887-4

Clim Dyn (2016) 47:1029–1047
DOI 10.1007/s00382-015-2887-4

Wintertime atmospheric response to Atlantic multidecadal variability: effect of stratospheric representation and ocean–atmosphere coupling

Yannick Peings[1] · **Gudrun Magnusdottir**[1]

Received: 29 April 2015 / Accepted: 17 October 2015 / Published online: 28 October 2015

Abstract The impact of the Atlantic multidecadal variability (AMV) on the wintertime atmosphere circulation is investigated using three different configurations of the Community Atmospheric Model version 5 (CAM5). Realistic SST and sea ice anomalies associated with the AMV in observations are prescribed in CAM5 (low-top model) and WACCM5 (high-top model) to assess the dependence of the results on the representation of the stratosphere. In a third experiment, the role of ocean–atmosphere feedback is investigated by coupling CAM5 to a slab-ocean model in which the AMV forcing is prescribed through oceanic heat flux anomalies. The three experiments give consistent results concerning the response of the NAO in winter, with a negative NAO signal in response to a warming of the North Atlantic ocean. This response is found in early winter when the high-top model is used, and in late winter with the low-top model. With the slab-ocean, the negative NAO response is more persistent in winter and shifted eastward over the continent due to the damping of the atmospheric response over the North Atlantic ocean. Additional experiments suggest that both tropical and extratropical SST anomalies are needed to obtain a significant modulation of the NAO, with small influence of sea ice anomalies. Warm tropical SST anomalies induce a northward shift of the ITCZ and a Rossby-wave response that is reinforced in the mid-latitudes by the extratropical SST anomalies through eddy–mean flow interactions. This modeling study supports that the positive phase of the AMV promotes the negative NAO in winter, while illustrating the impacts of the stratosphere and of the ocean–atmosphere feedbacks in the spatial pattern and timing of this response.

Keywords Atlantic multidecadal variability · North Atlantic Oscillation · Teleconnection · Cold extremes · Decadal forecasting · Jet stream · Rossby waves · Stratosphere–troposphere coupling · Ocean–atmosphere feedback

1 Introduction

The relationship between sea surface temperature (SST) anomalies and the large-scale atmospheric circulation has been thoroughly investigated in the literature, from observational analysis and modeling experiments. While two-way ocean–atmosphere interactions have been clearly identified in the tropics (for example in the case of the El Nino Southern Oscillation, e.g. Wang et al. 2004), it generally appears that at short time scales (weekly to interannual) the atmosphere drives the oceanic surface in the extratropics (Frankignoul 1985). The feedback from extratropical SST anomalies on the atmosphere exists (e.g., Peng and Whitaker 1999; Czaja and Frankignoul 1999; Magnusdottir et al. 2004, Deser et al. 2007; Kwon et al. 2011) but appears to be small with little predictive skill (Bretherton and Battisti 2000; Kushnir et al. 2002).

At longer timescales though, some predictability arises from multidecadal variability of the SST that is internally driven by ocean dynamics. In particular in the North Atlantic, the SST exhibits some long-term variability known as Atlantic multidecadal variability (AMV, Knight et al. 2006)

Electronic supplementary material The online version of this article (doi:10.1007/s00382-015-2887-4) contains supplementary material, which is available to authorized users.

✉ Yannick Peings
ypeings@uci.edu

[1] Department of Earth System Science, University of California, Irvine, CA 92697-3100, USA

or Atlantic multidecadal Oscillation (AMO, Kerr 2000). Since paleoclimatic data suggests that the periodicity varies in time, the multidecadal fluctuations of the North Atlantic SST are not a true oscillation (Gray et al. 2004; Knudsen et al. 2011) and the term AMV is more appropriate to describe this mode of variability. The forcing mechanism of the AMV is still unclear and subject to considerable debate. Several studies based on coupled ocean–atmosphere simulations (Delworth et al. 1993; Timmermann et al. 1998; Zhang and Wang 2013; Wang and Zhang 2013; Ba et al. 2014) have suggested that the AMV is tied to the Atlantic meridional overturning circulation (AMOC), the regional signature of the oceanic meridional overturning circulation (MOC, Kuhlbrodt et al. 2007). Various mechanisms have been identified for the AMOC, including wind-driven variability forced by atmospheric noise (e.g., Medhaug and Furevik 2011; Chen et al. 2015) or density anomalies in deep water formation regions (e.g., Jungclaus et al. 2005). According to these studies, the AMV is driven by internal oceanic dynamics and ocean–atmosphere interactions, but other works have emphasized the role of external forcings (solar, aerosols and volcanoes) in modulating the North Atlantic SST variability (Otterå et al. 2010; Booth et al. 2012; Knudsen et al. 2014). Observational measurements of the AMOC are too recent to investigate its impacts on long time scales, but coupled climate models suggest that a strong AMOC induces an increase of warm water transport from the tropics to the extratropics, resulting in the positive polarity of the AMV (e.g., Wang and Zhang 2013). Such an AMV-AMOC relationship is consistent with the pioneering work of Bjerknes (1964) who hypothesized that in the North Atlantic the atmosphere drives the SST variability on short time scales (up to interannual), while ocean dynamics is responsible for SST and potentially atmospheric variability at decadal/multidecadal time scales. This hypothesis is also verified by recent observational work that has investigated the relationship between surface heat fluxes and the North Atlantic SST (Gulev et al. 2013).

Investigating the impact of the AMV on the atmosphere is made difficult by the relative shortness of the instrumental record in comparison with the AMV periodicity, that is about 60–70 years in observations (Schlesinger and Ramankutty 1994; Kerr 2000). Therefore, climate model experiments are needed to investigate how the AMV influences the large-scale atmospheric circulation. In summer, the AMV has been found to influence the intensity of Atlantic tropical cyclones (e.g., Knight et al. 2006), the Amazonian and Sahel monsoon rainfall (e.g., Wang et al. 2012) and both North American and European summer climate (e.g., Sutton and Hodson 2005, 2007). In winter, the impact of the AMV is less evident but some recent studies have identified a link between the AMV and the North Atlantic Oscillation (NAO), also referred to as the Northern Annular Mode (NAM). The NAO/NAM is the leading mode of extratropical Northern Hemisphere (NH) atmospheric variability in winter. In these studies, the AMV-related SST anomalies induce a negative NAO/NAM response in winter in atmospheric general circulation models (AGCMs), that is associated with a southward shift of the North Atlantic storm track (Msadek et al. 2011; Omrani et al. 2014; Peings and Magnusdottir 2014a; Davini et al. 2015). Some coupled ocean–atmosphere simulations also support this relationship (Kavvada et al. 2013; Gastineau et al. 2013; Ba et al. 2014; Ruprich-Robert and Cassou 2014; Omrani et al. 2015), as do statistical analyses of observations/reanalyses from the 20th century (Peings and Magnusdottir 2014a). The AMV has also been found to modulate the probability of atmospheric blocking events in the North Atlantic sector (Häkkinen et al. 2011). Given the influence of NAO/NAM variability and blocking patterns on the temperature and precipitation of Eurasia and North America (Hurrell and van Loon 1997), the AMV-NAO linkage has important implications in terms of long-term predictability of climate over these regions. For example, the current positive polarity of the AMV is one factor that may have promoted the resurgence of extreme cold weather episodes over Europe and the eastern US in recent winters (Peings and Magnusdottir 2014a; Keenlyside and Omrani 2014), in addition to the possible influence of Arctic sea ice loss (e.g., Cohen et al. 2014; Peings and Magnusdottir 2014b).

Although the AMV-NAO linkage is suggested by several studies, the response of the wintertime atmospheric circulation to the AMV depends on the model configuration that is used. Hodson et al. (2010) did not find a significant response of the winter NAO using five different AGCMs with prescribed AMV-SST anomalies. However, Peings and Magnusdottir (2014a) found a significant NAO response with a similar SST forcing, but in a different AGCM (the latest version of the Community Atmospheric Model, CAM5). Unlike Hodson et al. (2010), the model output was also examined at a finer timescale (intraseasonal), which allowed us to identify a significant NAO response in late winter only. Msadek et al. (2011) also found a negative NAO response to a warm AMV using an AGCM (LMDZ) coupled to a slab mixed layer ocean model in the North Atlantic. Omrani et al. (2014) investigated the dependence of the NAO response on the representation of the stratosphere in ECHAM5. They only obtained a significant response of the NAO in the high-top version of their model (with 39 vertical levels and a lid at 0.01 hPa compared to 19 levels and a lid at 10 hPa in the low-top version). Therefore, the AMV–NAO relationship is dependent on the configuration of the model that is used, especially whether the coupling to the ocean is included and/or whether the stratosphere is resolved.

In this study, we revisit the AMV–NAO relationship with a set of numerical experiments using CAM5. This work is complementary to our Peings and Magnusdottir (2014a) paper that used only the low-top version of CAM5 with prescribed SST and sea ice. We assess the importance of ocean–atmosphere feedbacks and of the stratospheric representation in the AMV–NAO relationship by using two other configurations of CAM5: one where CAM5 is coupled to a slab ocean and another that includes a high-top stratosphere. Since the same tropospheric physics is used in each model version, we can highlight the differences that are related to each additional component. The paper is organized as follows. Section 2 describes the atmospheric model and the different experiments. Section 3.1 presents the surface forcing that is applied in each experiment and the resulting heat flux anomaly in winter. The atmospheric response is described in Sect. 3.2, with an emphasis on the NAO and the associated surface temperature anomalies. The response of the NAO and of the stratosphere are investigated at the intraseasonal time scale in Sect. 3.3. Section 3.4 discusses the presence of a tropical-extratropical teleconnection that partly explains the mid-latitude atmospheric response. Finally, Sect. 3.5 explores the role of tropical vs extratropical Atlantic SST anomalies, as previous studies have suggested that mid-latitude SST anomalies reinforce the response of the NAO and storm track to tropical Atlantic SST anomalies (Okumura et al. 2001; Drevillon et al. 2003; Peng et al. 2005; Sutton and Hodson 2007). A summary of the results and a discussion of the main findings are given in Sect. 4.

2 Methodology

The Community Atmospheric Model version 5 (CAM5) is an Atmospheric General Circulation Model developed by the National Center for Atmospheric Research (NCAR). CAM5 is the atmospheric component of the Community Earth System Model (CESM). Details about the model can be found in Neale et al. (2011). CAM5 is a low-top model with 30 vertical levels and a top at 2.2 hPa.

Two different configurations of the model are used. One with prescribed SST and sea ice concentration (SIC) and another with a slab ocean model (SOM) that has a seasonally varying mixed layer depth. The mixed layer depth and sea surface temperature are prognostic variables in the SOM and this model configuration allows for a fully interactive air-sea exchange. The slab ocean does not include any ocean dynamics, it only represents thermodynamical exchanges between the atmosphere and the mixed layer. To account for the lack of ocean dynamics in SOM, a heat flux (Q-flux) is included in the energy budget of the mixed layer. The Q-flux is estimated from a fully coupled ocean–atmosphere simulation and is used to compensate for the lack of heat transport and correct errors in the SST and sea ice simulations that are due to other missing processes. SOM is coupled to a thermodynamic sea ice model that controls snow depth, surface temperature, ice thickness and ice concentration, as well as internal energy in four layers for a single thickness category. Therefore SIC is a prognostic variable when SOM is used, i.e., SIC is no longer prescribed and it is interactive.

We also use the Whole Atmosphere Community Climate Model (WACCM), which is a high-top chemistry-climate model that extends in altitude to the lower thermosphere (approximately 140 km). WACCM is used with the CAM5 physics package and is thus referred to as WACCM5. Compared to CAM5, the model has 70 vertical levels with a lid at 5.1×10^{-6} hPa (approximately 140 km) and a fully interactive chemistry. WACCM also includes a parameterization of nonorographic gravity waves (Smith et al. 2014) and an option to prescribe the quasi-biennial oscillation (QBO) by relaxing equatorial zonal winds in the stratosphere. We use a relaxation towards a cyclic QBO that is deduced from observations (period of 28 months). It is important to highlight that the comparison between CAM5 and WACCM5 does not only reflect changes that are due to a higher vertical resolution in the stratosphere, but it also includes the impact of the interactive chemistry and of the QBO. Thus when we refer to the impact of the high-top stratosphere in the following of the paper, we actually refer to all the additional processes that are included in WACCM5 compared to CAM5.

In all our experiments, the horizontal resolution is 1.9° latitude and 2.5° longitude. Greenhouse gases and aerosol concentrations are representative of present-day conditions (year 2000). Three perturbation experiments are performed with the three different model configurations (Table 1, and description hereafter). Each experiment consists of two 81-year simulations representative of the positive and negative polarity of the AMV (AMV+ and AMV−), with 1 year of spin-up that is removed from the analysis. Seasonal means (for example December to March, DJFM) are obtained for each experiment by averaging the 80 remaining winter seasons. For each experiment, the output of the AMV− simulation is subtracted from the output of the AMV+ simulation to determine the response of the atmosphere to the AMV forcing. Thus we describe the response to the positive SST anomaly case by comparing it to the negative SST anomaly case, assuming linearity in the response to warm and cold AMV. We choose to not use a control run to compare our perturbation experiments so as to maximize the signal to noise ratio and estimate the consequence of a shift from a cold to a warm AMV (without considering a neutral state). Due to the short memory of the atmosphere, individual winters are considered statistically

Table 1 Description of the numerical experiments

Name	Configuration and description of the AMV forcing	Duration
LOW-TOP	CAM5 atmospheric model, prescribed SST/SIC 2 Simulations with positive and negative AMV forcing Annual cycle of monthly AMV SST/SIC anomalies superimposed on the 1979–2000 climatology (from HadISST observations)	80 years
HIGH-TOP	Identical to LOW-TOP, but with WACCM5 (high-top model with 70 vertical levels and interactive chemistry)	80 years
SLAB-OCEAN	CAM5 atmospheric model + mixed layer ocean model (SOM) Interactive SST in the Atlantic (from 30°S), interactive sea ice in the Arctic Prescribed SST/SIC everywhere else 2 simulations with positive and negative AMV forcing AMV heat flux anomalies estimated from AMV SST anomalies Annual cycle of AMV heat flux anomalies superimposed on the annual cycle of Q-flux in the Atlantic	80 years
All-NA	LOW-TOP configuration Annual cycle of monthly AMV SST anomalies superimposed on the 1979–2000 climatology (from HadISST observations, no sea ice forcing)	50 years
TR-only	LOW-TOP configuration Identical to All-NA but with tropical SST anomalies only (from 0 to 25°N)	50 years
ML-only	LOW-TOP configuration Identical to All-NA but with extratropical SST anomalies only (from 30°N to 75°N)	50 years

independent and a two-tailed Student t test is applied to assess the statistical significance of the differences between AMV+ and AMV−.

- "LOW-TOP" refers to the simulations that are performed using CAM5 with prescribed SST/SIC. A constant annual cycle of SST and SIC representative of the 1979–2000 climatology is prescribed everywhere except over the North Atlantic. Over the North Atlantic (from equator to 85°N), the annual cycle of the SST/SIC anomalies representative of the positive and negative AMV cycles are superimposed on the 1979–2000 climatological SST/SIC. The SST/SIC anomalies that are prescribed to the model (Fig. 1a, d shows wintertime anomalies) come from a composite analysis of the HadISST observations (Rayner et al. 2003) based on the value of the AMV index over 1953–2012. The composite analysis has been computed using the upper and lower quartiles of the AMV index as a threshold for warm and cold AMV. The 1953–2012 period was selected since it is a period for which SIC data exists in the North Atlantic sector (Walsh and Chapman 2001). The anomalies are detrended and low-pass filtered before computing the composites in order to isolate the decadal fluctuations of SST and SIC that are associated with the AMV. These simulations are similar to the ones that were performed and analyzed in Peings and Magnusdottir (2014a), except that they have been extended from 50 to 80 years.
- "HIGH-TOP" refers to the simulations that are performed with WACCM5 and prescribed SST/SIC. The SST/SIC boundary conditions are prescribed in exactly the same way as for LOW-TOP. The annual cycle of the boundary forcing is exactly the same (Fig. 1b, e). This experiment allows us to examine the dependence of our results on the representation of the stratosphere.
- "SLAB-OCEAN" refers to the simulation that uses CAM5 coupled to SOM. The SOM is only active in the Atlantic (from 40°S) and in the Arctic basin, with prescribed SST/SIC elsewhere (1979–2000 climatology). The thermodynamic sea ice model is therefore activated in the Arctic ocean and sea ice is interactive in this region only. Since SST is a prognostic variable in SOM, we do not prescribe SST anomalies in this model. Instead, the AMV forcing is included by adding a Q-flux anomaly in the SOM, similar to the method used by Zhang and Delworth (2006). The annual cycle of AMV Q-flux anomalies is added to the climatological annual cycle of Q-flux in the SOM. The AMV Q-flux anomalies are designed from the SST anomalies that are used in LOW-TOP and HIGH-TOP. The relationship between the Q-flux and SST anomalies may be written as $Q(t) = K \times SST_{AMV}(t)$ with

$$K = 15 \frac{\mathrm{W}}{\mathrm{K\ m^2}}$$

The symbol Q refers to Q-flux, $SST_{AMV}(t)$ is the monthly anomaly of SST corresponding to the positive or negative phase of the AMV. In addition with positive Q-flux anomalies in the North Atlantic, negative Q-flux anomalies are imposed in the South Atlantic (to 40°S) in order to simulate the northward Atlantic ocean heat transport across the equator and to avoid an unbalanced

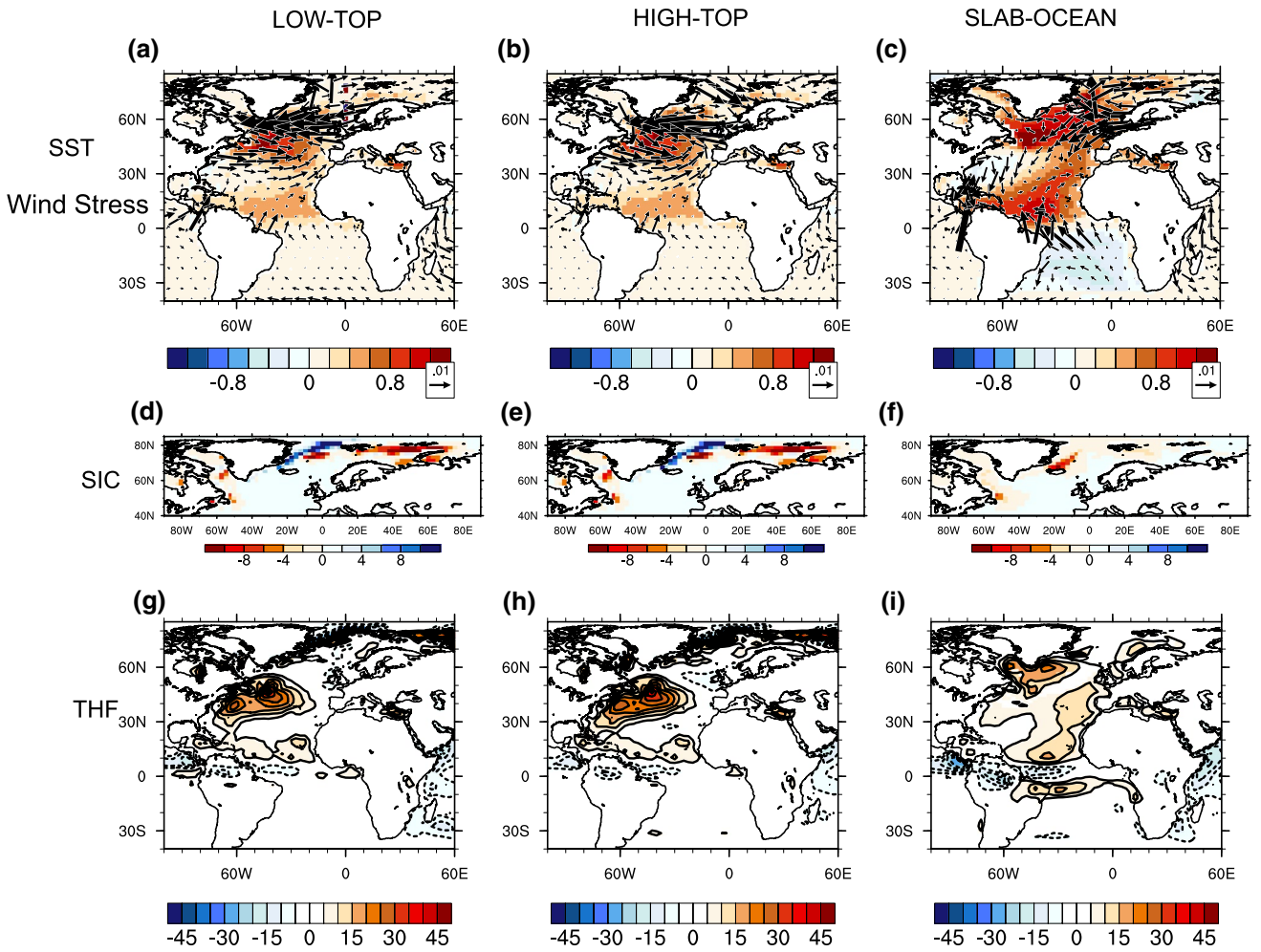

Fig. 1 **a** Prescribed DJFM sea surface temperature anomalies (°C) in LOW-TOP and response of the surface wind stress at the oceanic surface (N m^{-2}). **b** Same as **a** but for HIGH-TOP. **c** Response of the DJFM SST and surface wind stress to the Q-flux forcing imposed in SLAB-OCEAN. **d** Prescribed DJFM sea ice concentration anomalies (%) in LOW-TOP. **e** Same as **e** but for HIGH-TOP. **f** Response of the DJFM SIC in SLAB-OCEAN. **g** Response of the DJFM turbulent heat flux (THF, sensible + latent, W m^{-2}) in LOW-TOP. Significant anomalies at the 95 % confidence level are *shaded*. **h** Same as **g** but for HIGH-TOP. **i** Same as **g** but for SLAB-OCEAN

energy budget in our model. The value of the coefficient K has been chosen after running several sensitivity tests. It allows us to get a reasonable amplitude of SST anomalies in SLAB-OCEAN in comparison with the prescribed SST experiments. As the Q-flux anomalies are proportional to the SST anomalies that are prescribed in LOW-TOP and HIGH-TOP, their pattern is similar to the SST pattern in the North Atlantic (Fig. 1a, b). However, SST and SIC are now predicted variables such that the resulting SST/SIC anomalies are different in SLAB-OCEAN (Fig. 1c).

- In Sect. 3.5, three additional experiments of 50 years are analyzed: All-NA, TR-only and ML-only. These experiments are similar to LOW-TOP except with different SST forcings. AMV-SST anomalies are prescribed in the entire North Atlantic for All-NA, in the tropics only (between equator and 25°N) in TR-only and in mid-latitudes (between 30°N and 75°N) in ML-only. These experiments are useful to separate the role of tropical and extratropical SST anomalies in the atmospheric response. No sea ice anomalies are included in these experiments such that the comparison of All-NA to LOW-TOP allows us to estimate the importance of AMV-induced sea ice anomalies that are included in LOW-TOP and HIGH-TOP.

3 Results

3.1 Description of surface forcing and response of turbulent heat flux

Figure 1 shows the wintertime (DJFM) SST and SIC anomalies that are prescribed in LOW-TOP and HIGH-TOP

(Fig. 1a, b for SST, Fig. 1d, e for SIC). The prescribed SST anomalies are larger in the tropical Atlantic (~+0.4 °C) and south of Greenland in the vicinity of the Gulf stream and the subpolar gyre (up to +1.5 °C), in line with the increase of heat transport in this region during the positive phase of the AMV (Gulev et al. 2013). The imposed SIC anomalies are rather small, the main signal being the low sea ice values in the Barents-Kara Seas. For SLAB-OCEAN (Fig. 1c, f), SST and SIC are interactive variables thus the anomalies result from the response of the ocean–atmosphere coupled system to the Q-flux prescription in SOM. Figure 1g–i depicts the response of the total turbulent heat flux (sensible plus latent heat flux), i.e., the transfer of heat to the atmosphere that is induced by the oceanic forcing (positive values represent a gain of energy by the atmosphere). We do not show the radiative fluxes (shortwave + longwave) that have a small contribution compared to the turbulent heat fluxes. Wind stress anomaly vectors are superimposed onto the SST anomalies in Fig. 1a–c to illustrate the adjustment of the near-surface atmosphere to the forcing, that directly impacts the turbulent heat fluxes (according to bulk formulas, turbulent heat fluxes at the ocean–atmosphere interface are dependent on the temperature gradient, the humidity gradient and the surface wind speed, e.g. Park et al. 2005). The surface wind anomalies also indirectly impact the surface turbulent heat fluxes through temperature and humidity advection.

In LOW-TOP and HIGH-TOP, positive heat-flux anomalies are found in the area of maximum warm SST anomalies, in the Gulf stream region and off the coast of Newfoundland in mid-latitudes, and in the subtropical Atlantic (Fig. 1g–h). In mid-latitudes, heat flux anomalies are shifted southward compared to the SST anomalies as the cyclonic anomaly that develops in the surface wind field (Fig. 1a) reinforces (weakens) the turbulent heat fluxes south (north) of 50°N. In a coupled ocean–atmosphere system, the loss of energy from the ocean to the atmosphere would dampen the heat flux anomalies (Barsugli and Battisti 1998; Park et al. 2005), as verified in SLAB-OCEAN (Fig. 1i). This negative feedback is absent in LOW-TOP and HIGH-TOP, since SST is prescribed. Instead, the ocean acts as an infinite heat source for the atmosphere and a positive heat-flux feedback develops over the ocean in mid-latitudes, that reinforces the atmospheric anomaly and the surface wind stress response.

As expected, SLAB-OCEAN exhibits a very different behavior. SST anomalies are larger than for LOW-TOP and HIGH-TOP, especially to the east of the Q-flux forcing along the European/African coastline and in the Mediterranean and Norwegian Seas (the Q-flux forcing has the same pattern as the shading in Fig. 1a, b multiplied by the coefficient $K = 15$ W K^{-1} m^{-2}, see Methodology in Sect. 2). The larger SST anomalies possibly arise from a too large value of the coefficient K, as it is difficult to obtain a similar amplitude of SST anomalies in SLAB-OCEAN through the indirect method of imposing Q-flux anomalies in the oceanic mixed layer. Moreover, they are also a consequence of the inclusion of the ocean–atmosphere interaction in this experiment. As seen in the prescribed SST experiments (Fig. 1a, b), the warm SST anomaly in the mid-latitudes induces a cyclonic circulation near the oceanic surface, that is associated with a reduction of westerlies north of the center of the SST anomaly (north of 50°N) and an increase of westerlies south of 50°N. In SLAB-OCEAN, the SST adjusts to this atmospheric response by increasing where the surface wind stress weakens, and decreasing where it is reinforced. As a consequence, the SST anomaly tends to evolve towards the typical SST tripole pattern that is found to be forced by the negative phase of the NAO (Cayan 1992; Peng et al. 2005), which is found in the tropospheric response that is described in the next section. Note that only minor anomalies of sea ice concentration are found in this experiment (Fig. 1f). The response of Arctic sea ice to AMV is likely higher in nature (Day et al. 2012) and underestimated in our model, given that SOM does not represent horizontal and vertical oceanic movements that impact the distribution of sea ice in the Arctic.

Despite the larger amplitude of SST anomalies in SLAB-OCEAN, the resulting heat flux anomalies have a smaller amplitude, with a different pattern compared to LOW-TOP and HIGH-TOP (Fig. 1i). This is a result of including the ocean–atmosphere feedback that modifies the surface wind stress and the temperature/humidity gradients. For instance, as the ocean warms the saturation specific humidity at the air/sea interface increases, reducing the ocean–atmosphere humidity gradient that drives the latent heat flux. Compared to LOW-TOP and HIGH-TOP, the heat flux anomalies are shifted eastwards and are at maximum near the southern tip of Greenland and in the eastern Atlantic. As for heat flux anomalies, the response of the surface wind stress is also smaller over the North Atlantic (Fig. 1c). Compared to the prescribed-SST experiments, the ocean–atmosphere coupling that is included in SLAB-OCEAN thus results in increased (decreased) heat flux exchanges in the eastern (western) North Atlantic. This leads to a longitudinal shift the atmospheric response, as discussed in the next section.

3.2 Response of the North Atlantic Oscillation and of the surface temperature

Figure 2 shows the wintertime (DJFM) response of the atmospheric circulation at different levels in the atmosphere. Figures S1 and S2 are similar to Fig. 1 but show the early winter (DJ) and late winter (FM) anomalies respectively. The response in sea-level pressure (Fig. 2a–c) is shown along with the NAO pattern corresponding to each

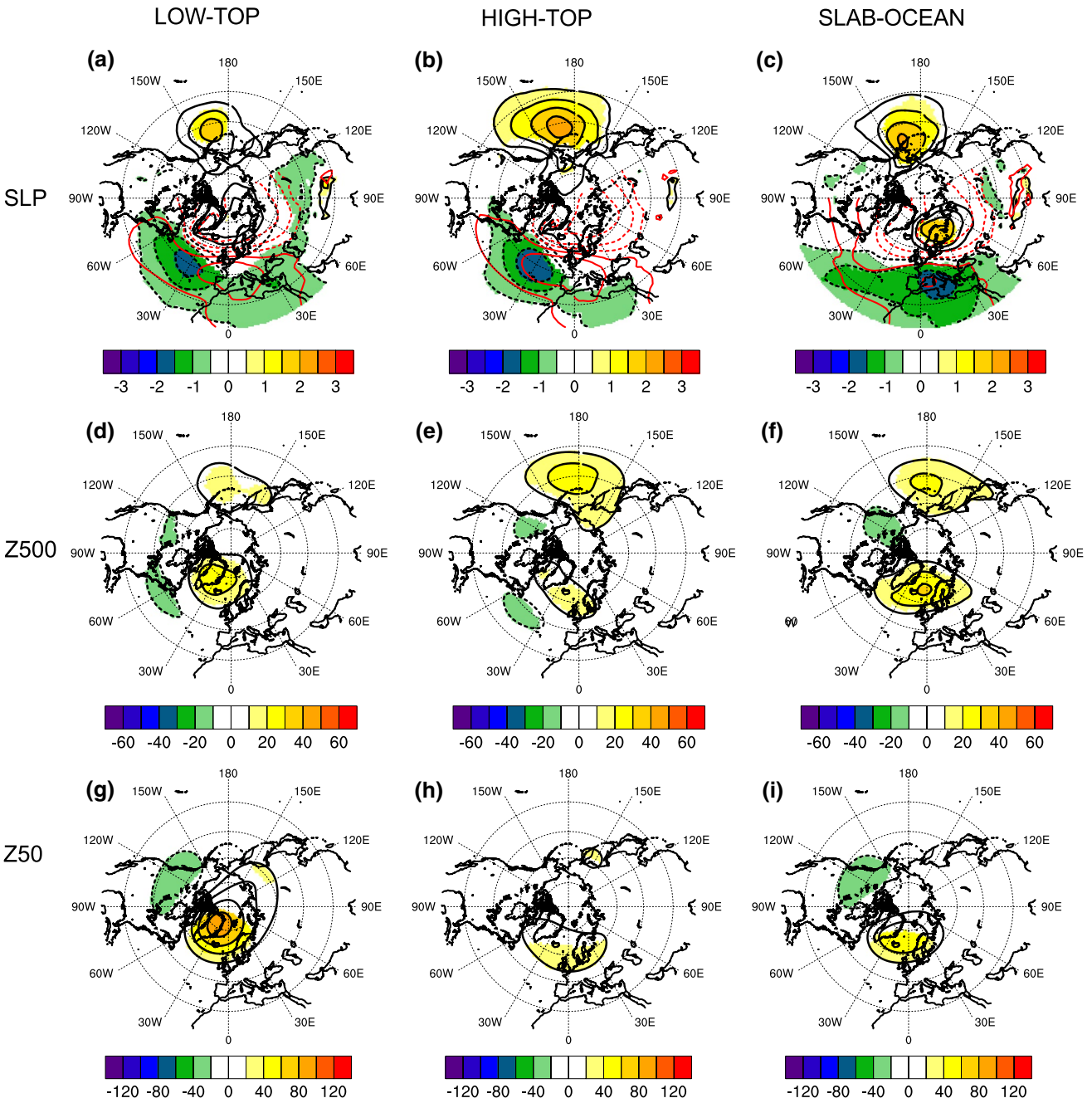

Fig. 2 **a** Response of the DJFM sea-level pressure (hPa) in LOW-TOP. Significant anomalies at the 95 % confidence level are *shaded*. *Red contours* represents the climatological NAO pattern in this experiment (contour interval 1 hPa). **b** Same as **a** but for HIGH-TOP. **c** Same as **a** but for SLAB-OCEAN. **d** Response of the DJFM 500 hPa geopotential height (m) in LOW-TOP. Significant anomalies at the 95 % confidence level are *shaded*. **e** Same as **d** but for HIGH-TOP. **f** Same as **d** but for SLAB-OCEAN. **g** Response of the 50 hPa geopotential height (m) in LOW-TOP. Significant anomalies at the 95 % confidence level are *shaded*. **h** Same as **g** but for HIGH-TOP. **i** Same as **g** but for SLAB-OCEAN

experiment (red contours, 1st EOF mode of North Atlantic/Europe DJFM SLP). In all configurations, the NAO pattern is consistent with the observed NAO (see Fig. S3 for comparisons of the NAO pattern in each configuration with observations) except for a eastward location of the maximum center of the northern lobe and a smaller amplitude of the southern lobe, especially in SLAB-OCEAN. The pattern of the SLP response in LOW-TOP and HIGH-TOP is reminiscent of the negative NAO. However, the negative pressure anomalies are located westward of the typical NAO pattern (Fig. 2a, b) and the statistical significance of the positive SLP anomalies in high latitudes is weak.

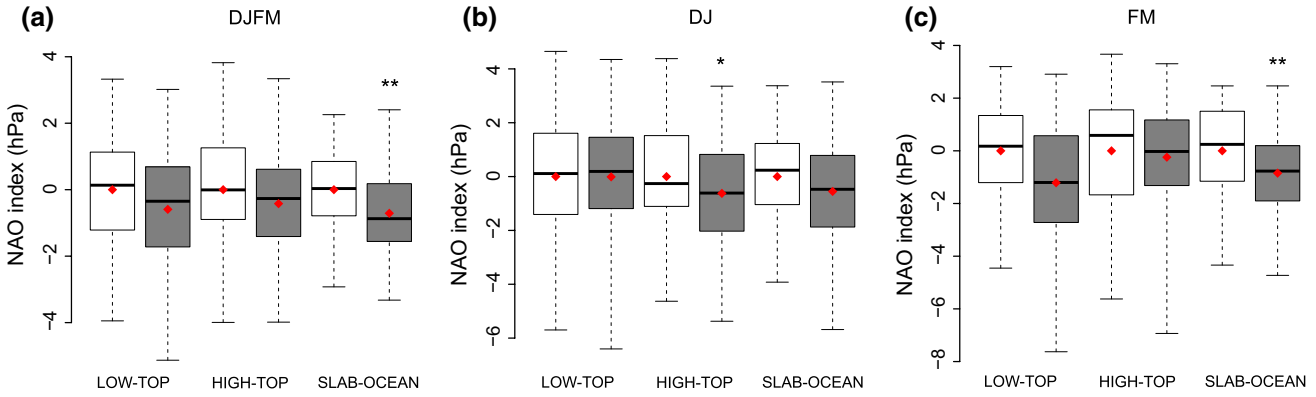

Fig. 3 **a** Distribution of the DJFM NAO index among the 80 winters of the simulations. Results are shown for the three configurations, *white boxplots* are for the AMV− simulation, *grey boxplots* are for the AMV+ simulation. *Boxplots* indicate the maximum, upper-quartile, median, lower-quartile and minimum of the distribution (*horizontal bars*). The mean of the distribution is shown by a *red diamond*, and *asterisks* indicate the significance level of the difference in the average NAO index between AMV− and AMV+: $*p < 0.1$; $**p < 0.05$ (two-tailed Student *t* test). **b** Same as **a** but for early winter (DJ). **c** Same as **a** but for late winter (FM)

As shown by the anomalies of the 500 hPa geopotential height (Fig. 2d–f), the response is asymmetric with a larger amplitude for the northern lobe of the NAO than for the southern lobe in the mid-troposphere. The sample size (80 winters) is sufficient to extract the AMV-driven atmospheric response (signal) from internal variability of the atmosphere (noise), since the negative NAO response remains stationary after 60 years of simulations (Figure S4). The larger and statistical significant signal that is found in the first 50 years of the experiment points out the danger of interpreting simulations that do not include large enough sample sizes.

The change in the distribution of the average NAO index between the 80 winters of each simulation is shown in Fig. 3. The mean (red diamonds), median, upper/lower quartile and maximum/minimum values (horizontal bars) are depicted on this plot, for the entire winter (DJFM, Fig. 3a) season as well as for early (DJ, Fig. 3b) and late winter (FM, Fig. 3c). The NAO index is computed by regressing the SLP anomalies onto the NAO pattern of each AMV- simulation (shown by red contours in Fig. 2a–c). A cold North Atlantic ocean is thus taken as the reference thereby the average NAO index is 0 in these simulations (cf Fig. 3). When the North Atlantic ocean is warm, the average DJFM NAO index decreases by −0.6 and −0.4 hPa for LOW-TOP and HIGH-TOP respectively, and the distribution shifts towards negative values (Fig. 3a). As pointed out in Peings and Magnusdottir (2014a), the response of the NAO occurs in late winter in LOW-TOP and is absent in early winter (Fig. 3b, c; Fig. S2). On the other hand, HIGH-TOP depicts a larger response in early winter than in late winter (Fig. 3b, c; Fig. S1). The maximum/minimum values of the distribution show that the intensity of extreme negative NAO increases during the positive polarity of the AMV, regardless of the season and/or model configuration. The extreme positive values are generally smaller.

In SLAB-OCEAN, the negative-NAO response (NAO index of −0.7 hPa, Fig. 3a) is qualitatively consistent with LOW-TOP and HIGH-TOP, although stronger in accordance with larger SST anomalies in this experiment. The main difference is the eastward shift of the NAO response, that is located over the continent rather than over the ocean (Fig. 2c). As expected from the heat flux response described in Sect. 3.1, the atmospheric response is damped over the North Atlantic ocean but reinforced over Europe and North Africa. As in other experiments, the response shows little resemblance to an equivalent barotropic structure in the vertical since a dipole is not found in the mid-troposphere (Fig. 2f). Finally, unlike LOW-TOP and HIGH-TOP, the NAO response is less subseason-dependent as it is present through the entire winter (Fig. 3a), although larger in late winter (Fig. 3c).

Figure 4 shows the associated anomalies of the 2-meter temperature. The three experiments exhibit a warming of the North Atlantic and the Greenland/Labrador Sea region, and a cooling of central Siberia (Fig. 4a–c). The cold anomaly found in central Siberia is interesting since a similar cold anomaly has been observed in recent years and has been attributed to the loss of Arctic sea ice, especially from the Barents–Kara Sea (Honda et al. 2009; Liu et al. 2012). We note that the AMV is able to force such an anomaly without any large sea ice anomalies in this region (especially in SLAB-OCEAN). This is consistent with Sato et al. (2014) that suggest that this relationship is a statistical artifact due to the combined influence of Gulf Stream SST anomalies onto both the Barents–Kara sea ice and the central Eurasia temperature. The overall temperature response is not strictly typical of a negative NAO anomaly, during

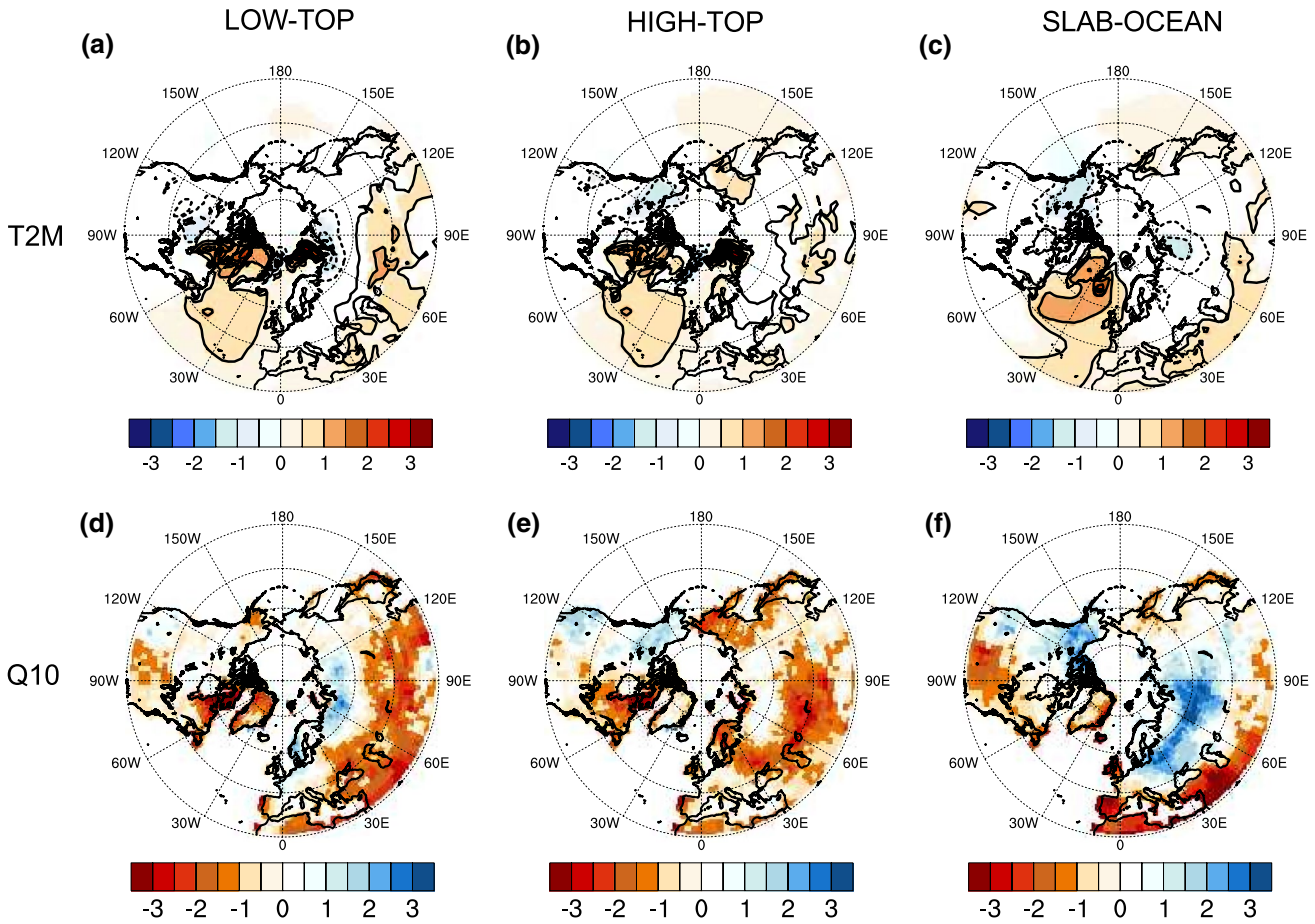

Fig. 4 **a** Response of the DJFM 2-m temperature (°C) in LOW-TOP. Significant anomalies at the 95 % confidence level are *shaded*. **b** Same as **a** but for HIGH-TOP. **c** Same as **a** but for SLAB-OCEAN. **d** Response of the DJFM percentage of cold days (%, from the 10th percentile of daily surface temperature) in LOW-TOP. **e** Same as d but for HIGH-TOP. **f** Same as **d** but for SLAB-OCEAN

which cold conditions are found over Europe and eastern North America (Hurrell and Van Loon 1997).

However, the impact of the NAO response is more visible in the change of cold extremes. Figure 4d–f show the change in percentage of wintertime days that are considered cold extreme days (using the 10th percentile of the daily temperature distribution of the AMV− simulation as a threshold for each grid point). An increase of cold extreme days is found over Eastern Europe and Siberia in LOW-TOP and SLAB-OCEAN. This is not the case in HIGH-TOP but once again this result is season dependent and tied to the timing of the NAO response. In early winter (Fig. S5b) when the response is maximum in HIGH-TOP, an increase of cold spell days is found over eastern Europe and western Siberia. In LOW-TOP, the increase in cold spell days is present over Eurasia and eastern North America in late winter only (Fig. S5d), in agreement with the results from Peings and Magnusdottir (2014a). In the absence of the NAO anomaly, the thermodynamical effect of a warm North Atlantic ocean dominates the dynamical effect and the surrounding continents are warmer (Fig. S5a and S5e). SLAB-OCEAN shows more consistency in the increase of cold extremes over Eurasia between early and late winter. It does not simulate any increase of cold extremes in the eastern US due to the shifted location of the NAO response in this experiment.

3.3 Response of the stratosphere and downward propagation of the signal

Omrani et al. (2014) found that the atmospheric response to the AMV is sensitive to the representation of the stratosphere. Indeed, a significant negative NAO response to warm AMV-SST anomalies is only obtained in the high-top version of their atmospheric model. They showed that the AMV forcing induces an anomalous planetary-wave propagation and a warming of the polar stratosphere in early winter that is followed by a downward propagation of the signal and a negative NAO in mid-winter. In our three experiments, we also observe a warming of the polar

stratosphere, which is consistent with their study although the amplitude is small (Fig. 2g–i). The weakening of the polar vortex is associated with upward propagation of planetary waves into the stratosphere in the North Atlantic sector (not shown). Unlike Omrani et al. (2014) though, our LOW-TOP model also simulates a weakening of the polar vortex, that is even of a larger amplitude than in HIGH-TOP. The discrepancy with their results might be related to the fact that CAM5 has a substantially greater vertical resolution than their low-top model ECHAM5 (30 levels in CAM5 compared to 19 in ECHAM5, with, respectively, 13 and 9 levels above 200 hPa), and a higher top level (2.2 hPa compared to 10 hPa). But more likely, this is explained by the turbulent mountain stress (TMS) parametrization that has been added in CAM5 and was absent in previous versions of CAM. When included, the TMS parametrization impacts the propagation of planetary waves into the stratosphere and improves the frequency of sudden stratospheric warming (SSW) events (Richter et al. 2010). Low-top models generally underestimate the frequency of SSWs (Charlton-Perez et al. 2013) due to the presence of a sponge layer with enhanced horizontal diffusion in the upper levels that inhibits the upward propagation of planetary waves. The sponge layer improves the climatology of the low-top models but leads to an underestimate of the stratospheric variability and the occurrence of SSWs. In CAM5, this bias is not very strong and SSWs are simulated: in the LOW-TOP experiment, we identify 25 SSW against 30 SSW in HIGH-TOP, based on a reversal of westerly to easterly winds in winter. This ability to simulate SSWs in both the low-top and high-top configurations might explain why our results show less dependence on the stratospheric representation than in Omrani et al. (2014).

As for the NAO, the timing of the response of the polar vortex differs between LOW-TOP and HIGH-TOP (Fig. S1g–i and S2g–i). To investigate the intraseasonal response in more detail, daily NAM anomalies (averages of geopotential height anomalies over the polar cap north of 65°N) are depicted in a time-pressure coordinate plot on Fig. 5a, c, e. This allows us to track NAM anomalies in the vertical and in time. In particular, they allow us to assess if any SSW event occurs during winter in the experiments. In order to verify how these polar cap anomalies project onto the NAO, we have also computed a daily NAO index for each winter season of the simulations by regressing the daily anomalies of the 1000 hPa geopotential height onto the corresponding NAO pattern (Fig. 5b, d, f). Z1000 is used instead of SLP that was not saved on the daily time scale. The NAO index is normalized and expressed in standard deviation instead of hPa as in Sect. 3.2, which explains the smaller amplitude of the NAO anomalies in Fig. 5. Red (blue) solid lines show the ensemble mean of the NAO index for the simulation for the positive (negative) AMV forcing. The envelope represents ±1 standard deviation of the inter-member variability, the maximum and minimum values are indicated by dashed lines. In line with results of the previous section, significant anomalies in the stratosphere are found in LOW-TOP and HIGH-TOP but with a different timing. In HIGH-TOP, a significant negative NAM anomaly appears in November, propagates downwards and reaches the surface in mid-January, while in LOW-TOP a similar response occurs in late winter and reaches the surface in late February and March. The values of the intraseasonal NAO index are consistent with the timing of the downward propagation of NAM anomalies. In the AMV+ simulation, the NAO tends to be negative in mid-winter in HIGH-TOP (Fig. 5d), in late winter in LOW-TOP (Fig. 5b). The inclusion of the high-top model has therefore an impact on the timing of the stratospheric response and following tropospheric anomalies. This result is consistent with Smith et al. (2014), that have found that the inclusion of WACCM changes the seasonality of SSWs in winter, with SSWs restricted to late winter in the low-top version. They attribute these changes to differences in the mean state of the model, especially concerning the strength of the westerly winds in the stratosphere that determine the sensitivity of the polar vortex to planetary wave breaking. Our perturbation experiments do not allow us to truly assess such differences in the mean state (it would necessitate a control experiment for each configuration). However, the polar night jet appears to be stronger in LOW-TOP than in HIGH-TOP, especially in early winter (not shown), which is one factor that can explain the different timing of the response from one configuration to the other.

An important finding is that the response in the stratosphere is small in SLAB-OCEAN during the entire winter (Fig. 5e) although this experiment has the largest NAO response. This suggests that the stratospheric response is not critical in the development of significant NAO anomalies at the surface, i.e. stratosphere–troposphere interactions are not the primary mechanism that can explain the response of the NAO to the AMV in our model. Rather, they seem to amplify the NAO response when the signal that emerges in the stratosphere reaches the surface. These results differ from Omrani et al. (2015) that found a stratospheric response in both a standalone and an ocean–atmosphere coupled version of their model. Nonetheless, this response was smaller in the coupled version, which is consistent with SLAB-OCEAN in suggesting that the ocean–atmosphere coupling dampens the response of the stratosphere.

In addition to highlighting intraseasonal variability, Fig. 5b, d, f also illustrates the amplitude of the forced NAO response compared to internal atmospheric variability. The forced response remains secondary compared to internal variability as suggested by the large spread of

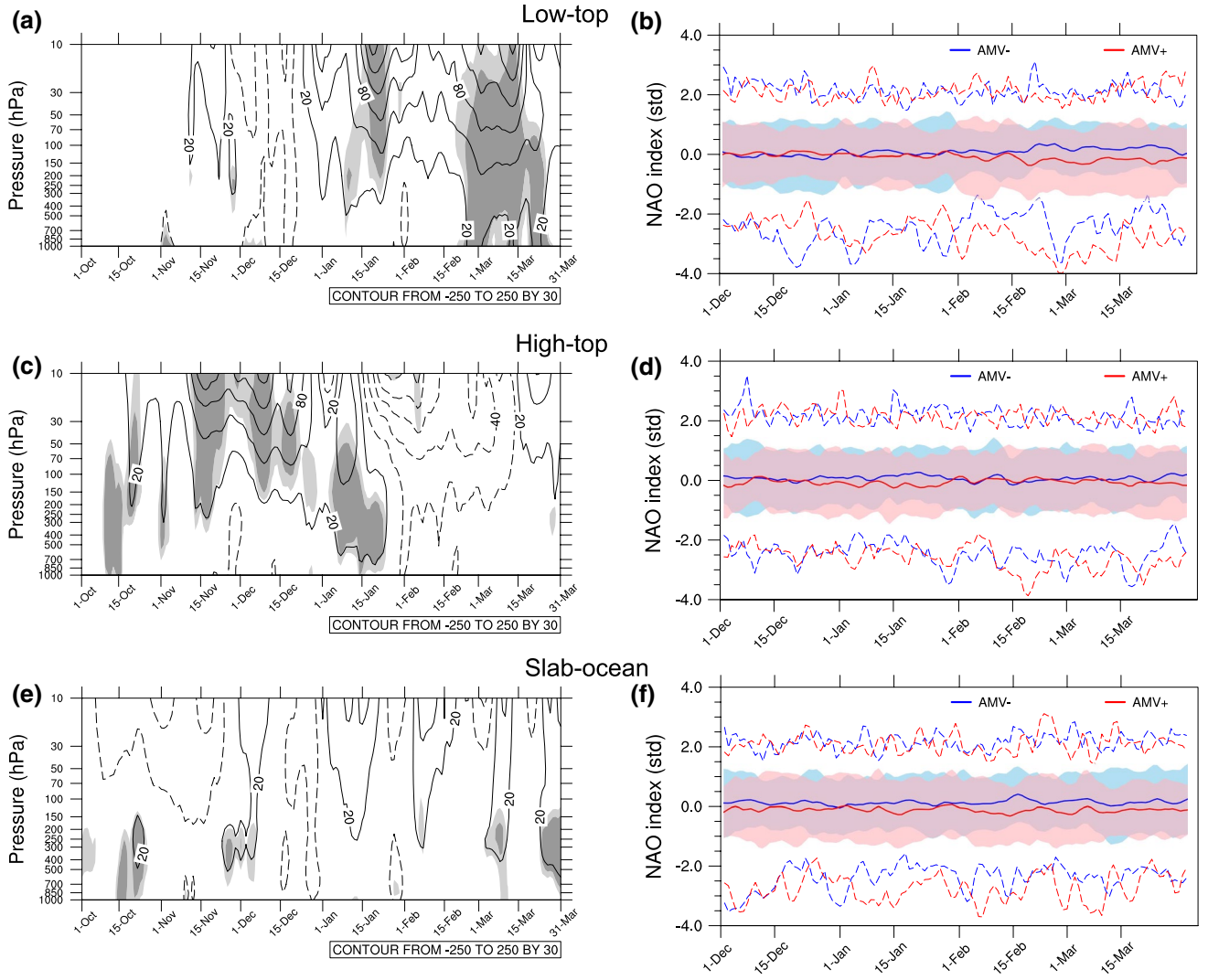

Fig. 5 **a** Time–pressure cross section of the daily polar cap response (m, geopotential averaged north of 65°N) in LOW-TOP. *Light* (*dark*) *shading* indicates significance at the 90 % (95 %) significance level. The contour interval is 30 m. **b** Daily anomalies of the NAO index (EOF-based index from the geopotential height at 1000 hPa) in LOW-TOP, for AMV+ (*red*) and AMV− (*blue*). The *solid line* represents the ensemble mean of the distribution (from 80 winters), the envelope shows the ±1 standard deviation interval and the *dashed lines* are the maximum/minimum values. **c** Same as **a** but for HIGH-TOP. **d** Same as **b** but for HIGH-TOP. **e** Same as **a** but for SLAB-OCEAN. **f** Same as **b** but for SLAB-OCEAN

the NAO index between the 80 winters in each simulation. Nevertheless, the average NAO index tends to be systematically lower when the AMV is warm, especially in SLAB-OCEAN where no seasonality is found in this response.

3.4 Shift of the ITCZ and generation of a Rossby wave

Figure 6 shows the response in precipitation. The three experiments simulate a northward shift of the Intertropical Convergence Zone (ITCZ). This response has been previously identified as a response to the warm phase of the AMV (e.g., Sutton and Hodson 2007; Ting et al. 2011) and is associated with the tropical Atlantic SST anomalies, as discussed in Sect. 3.5. In the mid-latitudes, precipitation increases with warm SST anomalies in LOW-TOP and HIGH-TOP (Fig. 6a, b), in agreement with the larger heat flux and atmospheric response over the ocean in these experiments. A positive feedback occurs between the precipitation and the dynamical response: the wind forcing increases the evaporation at the surface, leading to more precipitation that amplifies the anomalous cyclonic circulation through latent heat release in the free troposphere. This positive feedback leads to an overestimate of precipitation anomalies over the North Atlantic ocean in the absence of ocean–atmosphere coupling. In fact, the mid-latitude precipitation anomalies are absent or smaller in

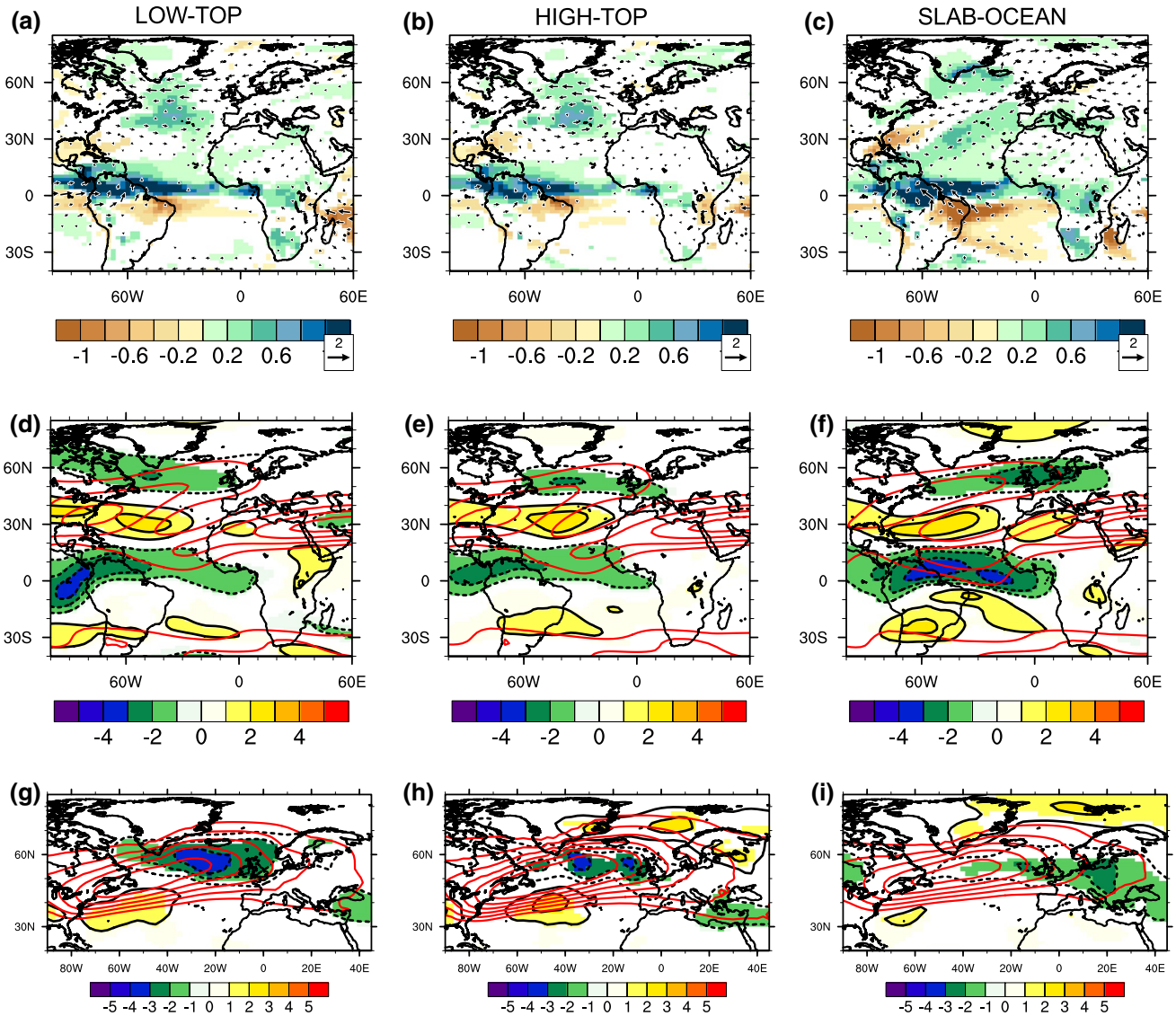

Fig. 6 **a** Response of the DJFM precipitation (mm day^{-1}, shading) and 850 hPa wind vectors (m s^{-1}) in LOW-TOP. Only responses that are significant at the 95 % confidence level are shown for the precipitation. **b** Same as a but for HIGH-TOP. **c** Same as a but for SLAB-OCEAN. **d** Response of the DJFM 200 hPa zonal wind (m s^{-1}) in LOW-TOP. Significant anomalies at the 95 % confidence level are *shaded*. *Red contours* represent the climatology (interval of 10 m s^{-1} between 20 and 50 m s^{-1}). **e** Same as **d** but for HIGH-TOP. **f** Same as **d** but for SLAB-OCEAN. **g** Response of the DJFM transient eddy activity (m) in LOW-TOP. Significant anomalies at the 95 % confidence level are *shaded*. *Red contours* represent the climatology (interval of 6 m between 30 and 60 m). **h** Same as **g** but for HIGH-TOP. **i** Same as **g** but for SLAB-OCEAN

SLAB-OCEAN (Fig. 6c), in which the ocean–atmosphere adjustment inhibits this positive feedback.

As expected from the negative phase of the NAO, the response of the 200 hPa zonal wind exhibits a tripole of zonal wind anomalies that corresponds to a merging of the North Atlantic polar front jet (eddy-driven) and the subtropical jet (thermally driven) (Fig. 6d–f). This tripole of zonal wind anomalies resembles a Rossby wave train that originates in the tropical Atlantic and propagates into the extratropics (this is clearly visible in streamfunction anomalies at 200 hPa, not shown since it is very consistent with U200 anomalies). A Rossby wave train that tilts eastward from the tropics to the northern extratropics is the typical large-scale atmospheric response to tropical SST anomalies (Hoskins and Karoly 1981). Such a response has been identified in numerous modeling studies that have investigated the influence of tropical SST anomalies on the atmosphere (e.g., Terray and Cassou 2002; Drevillon et al. 2003; Sutton and Hodson 2007). It is generated by anomalous upper-level divergence that results from enhanced evaporation and associated precipitation/latent heating anomalies in the free troposphere. In our experiments, the significant northward

shift of the ITCZ is the cause for the generation of upper-level divergence north of the equator and the generation of this Rossby wave train, as further demonstrated in the next section.

The coupling between atmosphere and ocean is stronger in the tropics such that the atmosphere is more sensitive to tropical SST anomalies than extratropical ones (see review by Kushnir et al. 2002). Even though their role is secondary compared to the influence of tropical SST, the extratropical SST anomalies have the potential to amplify the mid-latitude atmospheric response to tropical Atlantic SST anomalies through eddy–mean flow interactions (Peng et al. 2005; Sutton and Hodson 2007). Indeed, the transient eddies reinforce the large-scale circulation anomalies such as the NAO through eddy–mean flow feedbacks (Hoskins et al. 1983). The response of the transient eddy activity, defined as the standard deviation of filtered daily Z500 anomalies using a 2–6 day bandpass Lanczos filter, is shown in Fig. 6g–i. In LOW-TOP and HIGH-TOP, the transient eddy activity is reduced along the storm track, and slightly enhanced along its southern boundary. This is consistent with the response of the zonal flow and with the negative NAO signal. In SLAB-OCEAN, we note the absence of a significant response in transient eddy activity over the ocean (Fig. 6i) despite significant anomalies of the zonal flow at 200 hPa (Fig. 6f). Rather, the anomalies of the transient eddy activity are large over Europe where the NAO response is located (Fig. 2). This finding supports the central role of the eddy–mean flow feedback in modulating the amplitude and location of the NAO response. Since the respective role of tropical and extratropical SST anomalies are mixed up in the present experiments, their respective role in the atmospheric response cannot be isolated. Therefore, additional experiments have been performed that are discussed in the next section.

3.5 Additional experiments: role of tropical versus extratropical SST anomalies

In this section we examine the relative impact of tropical and extratropical SST anomalies in generating the NAO response that we have identified. Since the results are consistent between the three experiments in terms of the negative NAO response, we have performed additional experiments with the LOW-TOP configuration only as it is less demanding in term of computational costs. The All-NA (tropical plus extratropical forcing), TR-Only (tropical forcing) and ML-only (extratropical forcing) experiments are described in Sect. 2. All-NA is similar to LOW-TOP except that no sea ice anomalies are prescribed in the Arctic. We can therefore verify that the LOW-TOP response is mostly related to the SST anomalies and that the small sea ice anomalies play a secondary role. The experiments have been run for 50 years, which is sufficient to identify the mechanism that explains the influence of tropical and extratropical SST. The SST anomalies that are prescribed in these experiments are shown on Fig. 7a–c, together with the surface wind stress response (vectors). The SLP and 200 hPa zonal wind responses are shown in Fig. 7d–i.

First, we note that the response in All-NA is close to the one that is found in LOW-TOP (Fig. 7d, g vs Fig. 2a, g), confirming that the prescribed sea ice anomalies have a small influence in the average wintertime response of LOW-TOP. The influence of sea ice anomalies is discernible in late-winter only when LOW-TOP exhibits a larger response than All-NA (not shown), but this could also be an effect of the sample size (80 years in LOW-TOP against 50 years in All-NA). TR-Only reproduces the low SLP anomalies in the North Atlantic. The Rossby wave pattern that was identified in LOW-TOP is found in the zonal wind anomalies (Fig. 7h), confirming the role of tropical SST anomalies in generating this large-scale circulation anomaly. However, the U200 anomalies have a smaller amplitude than in All-NA and they are not statistically significant in mid-latitudes. On the other hand, ML-only exhibits a dipolar anomaly of U200 in the mid-latitudes, but with a small amplitude compared to All-NA (Fig. 7i). An interesting finding is that the combined response to tropical and extratropical SST anomalies is not linear, i.e. the response in All-NA is larger than the sum of the TR-Only response and the ML-only response. Therefore, a feedback mechanism is acting to amplify the response to extratropical SST anomalies in the presence of tropical SST anomalies (and vice versa), such that both part of the forcing are needed to obtain the significant negative-NAO pattern in our model. This result is consistent with that of Sutton and Hodson (2007) in modeling experiments with prescribed tropical and extratropical AMV SST anomalies. This is also consistent with Peng et al. (2005), although their extratropical SST anomalies were not prescribed but resulted from the response of a slab ocean model coupled to the atmosphere in the North Atlantic basin only. In contrast, Davini et al. (2015) found that the NAO response was exclusively forced by the tropical component of AMV-SST anomalies, emphasizing that the respective role of tropical versus extratropical SST is model-dependent.

The extratropical Atlantic SST reinforces the response that is generated by the tropical forcing by modifying the baroclinicity and storm track activity in the mid-latitudes. The change in transient eddy activity feeds back on the zonal mean flow and induces significant perturbations to the jet stream (Peng et al. 2005). This mechanism is verified in our experiments. Figure 8 shows the response of the transient eddies and of the E-vector (**E**) and its divergence (Hoskins et al. 1983). **E** gives a description of the transient eddy forcing upon the local time-mean

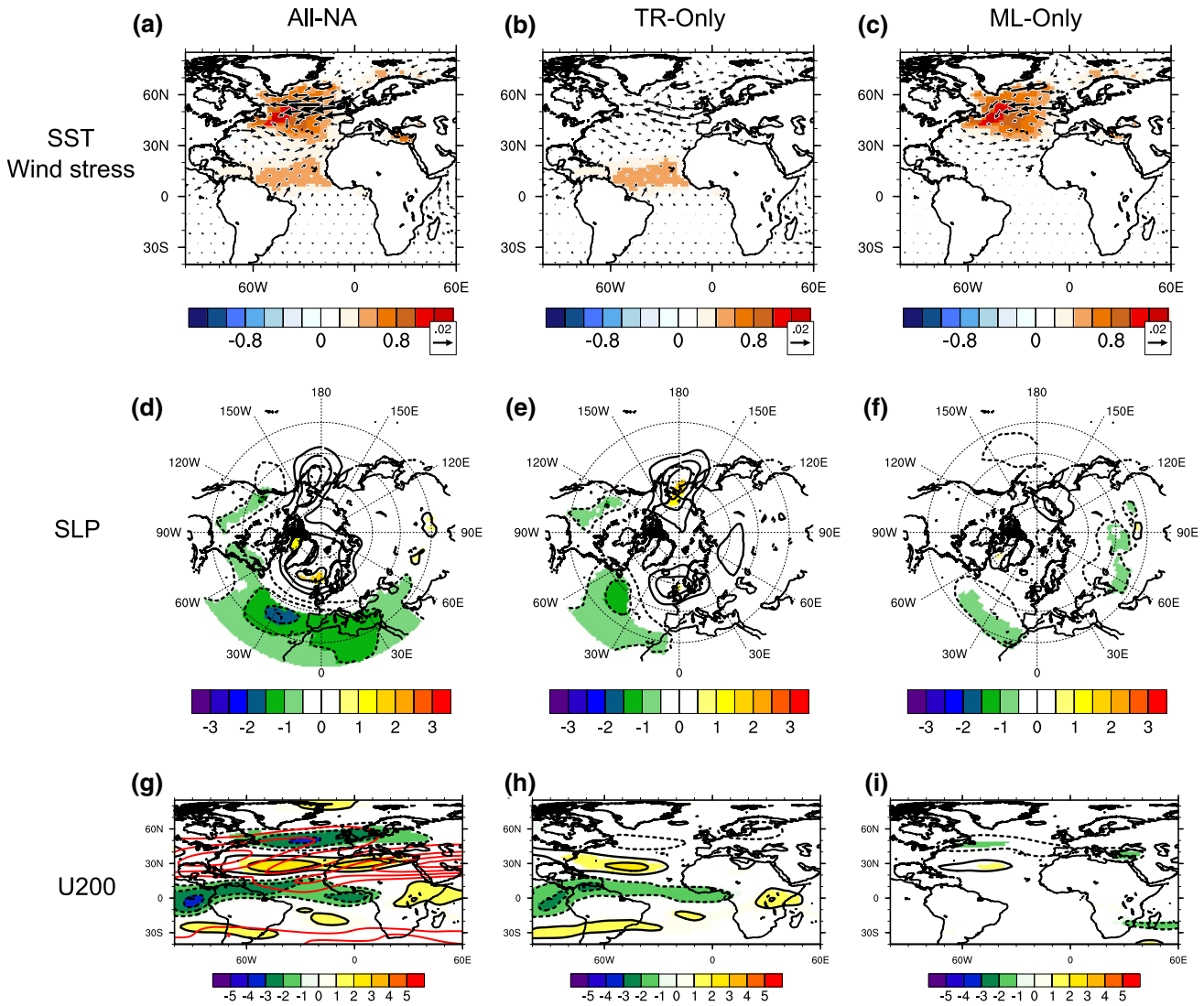

Fig. 7 **a** Prescribed DJFM sea surface temperature anomalies (°C) in All-NA and response of the surface wind stress at the oceanic surface (N m^{-2}). **b** Same as **a** but for TR-Only. **c** Same as **a** but for ML-Only. **d** Response of the DJFM sea-level pressure (hPa) in All-NA. Significant anomalies at the 95 % confidence level are *shaded*. **e** Same as **d** but for TR-Only. **f** Same as **d** but for ML-Only. **g** Response of the DJFM 200 hPa zonal wind (m s^{-1}) in All-NA. Significant anomalies at the 95 % confidence level are *shaded*. *Red contours* represent the climatology (interval of 10 m s^{-1} between 20 and 50 m s^{-1}). **h** Same as **g** but for TR-Only. **i** Same as **g** but for ML-Only

flow. It is computed from the synoptic components of the horizontal wind, after filtering with a 2–6 days band-pass Lanczos filter: $E = (\overline{v'^2 - u'^2}, \overline{-u'v'})$. **E** is in the direction of the group velocity of the transient eddies relative to the local time-mean flow. The divergence of **E** depicts the eddy-induced accelerations of the zonal wind due to barotropic processes. In TR-Only (Fig. 8b, e), the response in eddy transient activity and **E** is small and with little significance. In ML-only, a decrease of the transient activity is found along the Atlantic storm track (Fig. 8c) that induces a weakening of the westerly circulation as illustrated by the convergence of **E** along the storm track in Fig. 8f. The extratropical SST anomalies are thus responsible for perturbing the transient eddy activity, that is an amplifying mechanism in the response of the mid-latitude atmospheric circulation over the North Atlantic. This result demonstrates the importance of extratropical SST anomalies, since tropical and extratropical SST anomalies must coincide to obtain a significant modulation of the wintertime NAO in the LOW-TOP configuration. Further experiments would be needed to verify that the same mechanism is at work in the other model configurations. Nevertheless, this is presumably the case as both HIGH-TOP and SLAB-OCEAN exhibits a decrease of the transient eddy activity near the core of the NAO response (Fig. 6h, i).

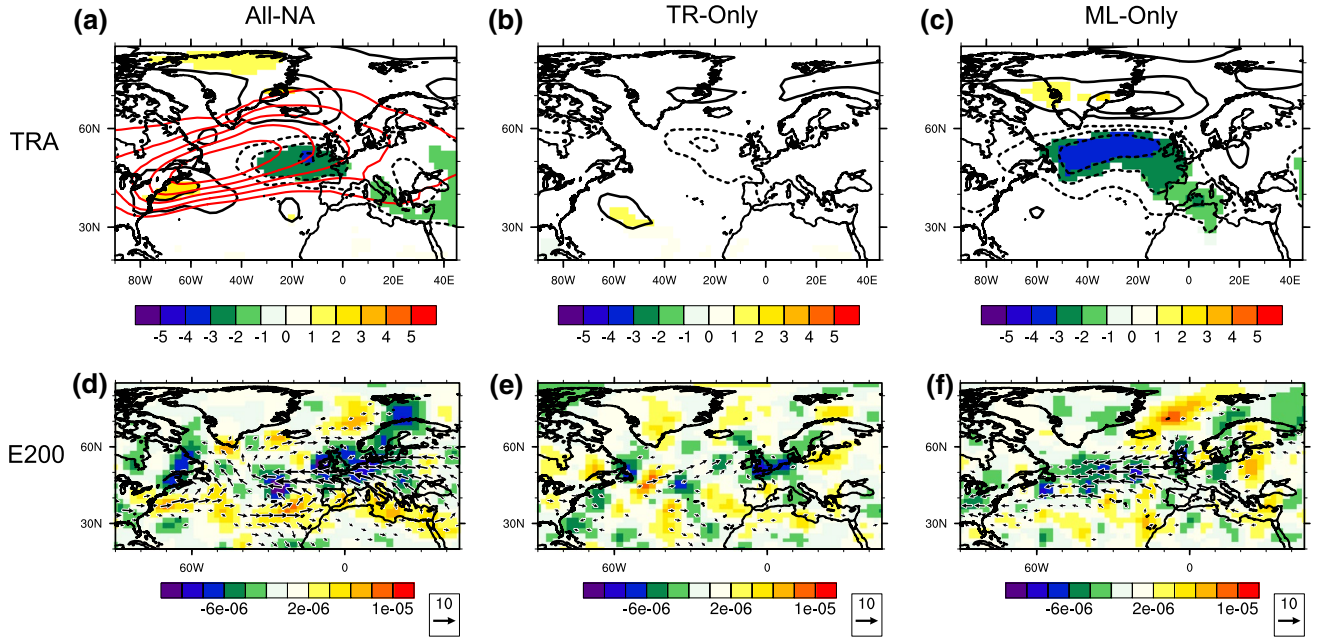

Fig. 8 **a** Response of the DJFM transient eddy activity (m) in All-NA. Significant anomalies at the 95 % confidence level are *shaded*. *Red contours* represent the climatology (interval of 6 m between 30 and 60 m). **b** Same as **a** but for TR-Only. **c** Same as **a** but for ML-only. **d** Response of **E** (*arrows*, $m^2\ s^{-2}$) and of its divergence (*shading*, $m\ s^{-2}$) in All-NA. **e** Same as **d** but for TR-Only. **f** Same as **d** but for ML-Only

4 Conclusion

In this paper we have used three different configurations of CAM5 (low-top, high-top and low-top coupled to a slab-ocean) to examine the response of the wintertime atmospheric circulation to the AMV. We have also examined the relative importance of tropical SST, extratropical SST and sea ice anomalies in the response. Here are our main conclusions:

- In the three configurations, the response to a warm AMV resembles the negative phase of the NAO, although the response is somewhat asymmetrical since the high pressure anomalies in high-latitudes are small compared to the mid-latitude low pressure anomalies. The timing of the NAO response is different between the three experiments, with a larger response in late winter in LOW-TOP, early winter in HIGH-TOP and a somewhat persistent response in SLAB-OCEAN. The NAO anomaly is associated with a southward shift in the upper-level North Atlantic polar front jet stream and the transient eddy activity along the storm track. The response in continental temperature is less consistent between the three experiments, but cold extreme events tend to increase over Europe/Asia when the negative NAO anomaly is maximum.
- Unlike in Omrani et al. (2014), that found a strong sensitivity of the results to the representation of the stratosphere, the use of the high-top model does not fundamentally change the results. In fact, LOW-TOP also simulates a polar warming of the stratosphere in response to a warm North Atlantic ocean, that promotes a negative NAO at the surface through stratosphere–troposphere interactions. This is likely related to the inclusion of the turbulent mountain stress parametrization in CAM5 (Richter et al. 2010) that has an impact on the upward propagation of planetary waves and on stratospheric variability. The remarkable ability of CAM5 to simulate SSW events in comparison with typical low-top models (Charlton-Perez et al. 2013) is probably related to the TMS parametrization. This will have to be confirmed in dedicated experiments. The representation of the stratosphere has an influence on the timing of the NAO response. This different timing (late winter in LOW-TOP, early winter in HIGH-TOP) is due to an earlier occurrence of the polar warming in the stratosphere in HIGH-TOP, that is followed by downward propagating NAM anomalies. But all in all, the stratospheric response is rather small and results from the SLAB-OCEAN experiment suggest that it is not the primary driver of the NAO response. Indeed, SLAB-OCEAN does not exhibit any significant anomalies in

the stratosphere, even though this is the experiment that simulates the largest response of the NAO. In light of this finding, the AMV–NAO teleconnection exists independently of stratospheric processes, but stratosphere–troposphere interactions can amplify the surface signature of the NAO several weeks after the occurrence of a warming of the polar stratosphere.

- When SST anomalies are prescribed, a positive feedback takes place between the heat flux and the surface wind stress in mid-latitudes. This leads to an amplified response of the atmospheric circulation over the North Atlantic. Our SLAB-OCEAN experiment shows that when a simple ocean–atmosphere coupling is included, this feedback is damped resulting in a smaller atmospheric response over the mid-latitude ocean. A significant negative-NAO response is still present but it is shifted eastward over the European and African continents. This response is associated with tropical SST anomalies that result from the Q-flux forcing. Large amplitude SST anomalies also develop in the eastern North Atlantic, beyond the area of the original Q-flux forcing, and these are reminiscent of the tripole-like SST pattern that is generally associated with the NAO (e.g. Cayan 1992). SLAB-OCEAN suggests that accounting for ocean–atmosphere coupling in such sensitivity experiments is important (Barsugli and Battisti 1998; Sutton and Mathieu 2002), but that it does not dramatically change the overall nature of the response (i.e., negative NAO and northward shift of the ITCZ in the tropical Atlantic). Note that the results from SLAB-OCEAN are dependent on the method that is used to prescribe the heat flux anomalies as Q-flux anomalies in SOM. Prescribing the average heat flux response from LOW-TOP or HIGH-TOP would allow a better consistency between the heat flux forcing among the three experiments. However, this method is also limited by biases in the net heat flux response that is found in the prescribed-SST experiments. An additional experiment (not shown in this paper) using such a methodology gives results that are quite similar to the prescribed-SST experiments, again suggesting that our results do not strongly depend on the representation of the ocean–atmosphere coupling in the North Atlantic.
- As noted in previous studies (Peng et al. 2005; Sutton and Hodson 2007), both extratropical and tropical SST anomalies play a role in the NAO response. A non-linear interaction exists in mid-latitudes, such that the sum of the individual response fields to each SST forcing is considerably smaller than the response to both forcings. The tropical SST anomalies induce a northward shift of the ITCZ by modifying the interhemispheric gradient of SST. The resulting perturbation in deep convection and precipitation leads to some upper-level divergence that generates a Rossby wave train into mid-latitudes, in agreement with previous studies (e.g. Okumura et al. 2001; Drevillon et al. 2003; Peng et al. 2005). The mid-latitude atmospheric response is then amplified by the influence of mid-latitude SST anomalies. Warm SST anomalies generate large heat flux anomalies in the Gulf stream region that modify the baroclinicity in the troposphere and decrease the eddy transient activity along the storm track. The anomalous transient activity feeds back on the zonal mean flow and leads to a shift in the mid-latitude jet stream and to a negative NAO response. The additional forcing due to mid-latitudes SST anomalies is only effective in the presence of the Rossby wave train driven by the tropical response. The overlap between the SLP anomalies and the decrease in transient eddy activity in SLAB-OCEAN further supports the role of eddy–mean flow feedbacks in shaping the NAO response. Caution must be exercised when interpreting the influence of tropical SST anomalies from the AMV on the atmospheric circulation. In fact, it is likely that tropical SST anomalies associated with the AMV are not driven by the ocean dynamics, but are induced by NAO anomalies associated with the AMV through modulation of the trade winds (Xie and Carton 2004). Even if tropical SST anomalies constitute a response rather than a driver of the NAO, our simulations suggest that they exert a positive feedback on the NAO and reinforce the atmospheric circulation that generates them.
- An interesting finding of these experiments is the presence of significant high pressure anomalies in the North Pacific (weakening of the Aleutian Low) (e.g., Fig. 2a–f). A North Pacific response has also been found in response to the warm North Atlantic SST anomalies of the 2012–2013 winter (Peings and Magnusdottir 2015) and in previous studies that have explored the atmospheric response to AMV-SST anomalies (Sutton and Hodson 2007; Msadek et al. 2011). Okumura et al. (2009) also identified a deepening of the Aleutian low in "water-hosing" experiments that aim to explore the impact of a weakening of the AMOC in coupled ocean–atmosphere GCMs. They attributed two-thirds of the Aleutian low response to the tropical Atlantic SST, presuming a remote impact of the tropical Atlantic SST over the North Pacific atmospheric circulation through the propagation of Rossby waves along the South Asian subtropical jet (as suggested by Haarsma and Hazeleger 2007). In this paper we have made the choice of focusing on the Atlantic portion of the atmospheric response, but future work will be dedicated to understanding the physical mechanisms behind this connection between the AMV and the North Pacific atmospheric circulation.

The consistency of our results among the three model configurations suggests that the influence of the AMV on the wintertime NAO (as well as on the ITCZ) is robust. As pointed out in Peings and Magnusdottir (2014a), the AMV should therefore be considered a forcing mechanism that may have driven the resurgence of negative NAO winters in recent years. Without that mechanism, the role of other factors, in particular the role of rapid Arctic sea ice decline (Vihma et al. 2014) may be overestimated, especially since the AMV directly influences the Arctic sea ice distribution (Day et al. 2012; Sato et al. 2014). Still, it is important to remember that, the same as for Arctic sea ice decline, the forcing mechanisms associated with the AMV are quite small compared to internal variability of the atmosphere (Wallace et al. 2014). This is the case in our experiments, in which the forced NAO signal is statistically significant but small compared to the atmospheric noise (as illustrated in Fig. 5). The dependence of the atmospheric response to the QBO has not been discussed in the present study due to limited sample sizes when partitioning the winter seasons into east and west QBO (<40 years in each case). However, it is known that the QBO influences the polar vortex dynamics (e.g. Watson and Gray 2014) and thus the sensitivity of the extratropical atmosphere to surface forcings such as Siberian snow anomalies (Peings et al. 2012) or SST anomalies (Garfinkel and Hartmann 2010). Preliminary analyses of our simulations suggest that the AMV response indeed depends on the QBO timing, with a weaker polar vortex and a larger NAO/NAM response when the QBO is easterly. This is an encouraging result since its suggests that more predictability could be gained from the AMV during years with an east QBO. However, longer simulations will have to be performed to ensure the robustness of this result and to detail the underlying physical mechanisms.

Our results will have to be supported by further experiments using models of different complexities to verify that they are robust. As we have used a simple slab-ocean model to represent the thermodynamic exchanges between the atmosphere and the ocean, we have ignored the role of ocean dynamics in modulating the response, and in particular the influence of the AMOC. Investigating the interactions between the AMOC, AMV and the atmospheric circulation necessitates the use of a fully coupled GCM. Recent studies that have used long-term simulations from the Coupled Model Intercomparison Project (CMIP) database have identified various lead-lag relationships between the AMOC, AMV and atmospheric modes such as the NAO. In particular, a negative NAO signal generally follows the positive AMV some years later in certain CMIP5 models (e.g., Gastineau et al. 2013; Ruprich-Robert and Cassou 2014), in agreement with our findings. Although the CMIP5 models exhibit significant biases in simulating the AMV that limits their usefulness in addressing this question (Zhang and Wang 2013; Ba et al. 2014), such detailed analyses of coupled GCMs simulations will undoubtedly improve our understanding of the influence of the AMV on the atmospheric circulation.

Acknowledgments This work was supported by NSF Grant AGS-1407360. We acknowledge high-performance computing support from Yellowstone (ark:/85065/d7wd3xhc) provided by NCAR's CISL, sponsored by the NSF. We are grateful to Noel Keenlyside, Nour-Eddine Omrani, Clara Deser and Lantao Sun for valuable discussions that have helped us better interpret the results of our experiments. Thanks are also due to Yi-Hui Wang for testing CAM with the slab ocean configuration. We finally thank two anonymous reviewers and the editor for their helpful comments and suggestions.

References

Ba J, Keenlyside NS, Latif M, Park W, Ding H, Lohmann K, Mignot J, Menary M, Ottera OH, Wouters B, SalasyMelia D, Oka A, Bellucci A, Volodin E (2014) A multi-model comparison for Atlantic multidecadal variability. Clim Dyn. doi:10.1007/s00382-014-2056-1

Barsugli JJ, Battisti DS (1998) The basic effects of atmosphere–ocean thermal coupling on midlatitude variability. J Atmos Sci 55:477–493

Bjerknes J (1964) Atlantic air–sea interaction. Adv Geophys 10:1–82

Booth BBB, Dunstone NJ, Halloran PR, Andrews T, Bellouin N (2012) Aerosols implicated as a prime driver of twentieth-century North Atlantic climate variability. Nature. doi:10.1038/nature10946

Bretherton CS, Battisti DS (2000) An interpretation of the results from atmospheric general circulation models forced by the time history of the observed sea surface temperature distribution. Geophys Res Lett 27:767–770

Cayan DR (1992) Latent and sensible heat flux anomalies over the northern oceans: driving the sea surface temperature. J Phys Oceanogr 22(859–881):17

Charlton-Perez AJ, Baldwin MP, Birner T, Black RX, Butler AH, Calvo N, Davis NA, Gerber EP, Gillett N, Hardiman S, Kim J, Krüger K, Lee Y-Y, Manzini E, McDaniel BA, Polvani L, Reichler T, Shaw TA, Sigmond M, Son S-W, Toohey M, Wilcox K, Yoden S, Christiansen B, Lott F, Shindell D, Yukimoto S, Watanabe S (2013) On the lack of stratospheric dynamical variability in low-top versions of the CMIP5 models. J Geophys Res Atmos 118:2494–2505. doi:10.1002/jgrd.50125

Chen H, Schneider EK, Zhu Z (2015) Mechanisms of internally generated decadal-to-multidecadal variability of SST in the Atlantic Ocean in a coupled GCM. DOI, Clim Dyn. doi:10.1007/s00382-015-2660-8

Cohen J, Screen JA, Furtado JC, Barlow M, Whittleston D, Coumou D, Francis J, Dethloff K, Entekhabi D, Overland J, Jones J (2014) Recent Arctic amplification and extreme mid-latitude weather. Nat Geosci 7:627–637

Czaja A, Frankignoul C (1999) Influence of the North Atlantic SST on the atmospheric circulation. Geophys Res Lett 26:2969–2972

Davini P, von Hardenberg J, Corti S (2015) Tropical origin for the impacts of the Atlantic Multidecadal Variability on the Euro-Atlantic climate. Environ Res Lett 10:094010. doi:10.1088/1748-9326/10/9/094010

Day JJ, Hargreaves JC, Annan JD, Abe-Ouchi A (2012) Sources of multi-decadal variability in Arctic sea ice extent. Environ Res Lett 7:034011. doi:10.1088/1748-9326/7/3/034011

Delworth T, Manabe S, Stouffer RJ (1993) Interdecadal variations of the thermohaline circulation in a coupled ocean–atmosphere model. J Clim 6:141–157

Deser C, Tomas RA, Peng S (2007) The transient atmospheric circulation response to North Atlantic SST and sea ice anomalies. J Clim 20:4751–4767

Drevillon M, Cassou C, Terray L (2003) Model study of the North Atlantic region atmospheric response to autumn tropical atlantic sea-surface-temperature anomalies. Q J R Meteorol Soc 129:2591–2611. doi:10.1256/qj.02.17

Frankignoul C (1985) Sea surface temperature anomalies, planetary waves, and air-sea feedback in the middle latitudes. Rev Geophys 23(4):357–390. doi:10.1029/RG023i004p00357

Garfinkel CI, Hartmann DL (2010) Influence of the quasi-biennial oscillation on the North Pacific and El Niño teleconnections. J Geophys Res 115:D20116. doi:10.1029/2010JD014181

Gastineau G, D'Andrea F, Frankignoul C (2013) Atmospheric response to the North Atlantic Ocean variability on seasonal to decadal time scales. Clim Dyn 40(9–10):2311–2330

Gray ST, Graumlich LJ, Betancourt JL, Pederson GT (2004) A tree-ring based reconstruction of the Atlantic Multidecadal Oscillation since 1567 A.D. Geophys Res Lett 31:L12205. doi:10.1029/2004GL019932

Gulev SK, Latif M, Keenlyside N, Park W, Koltermann KP (2013) North Atlantic Ocean control on surface heat flux on multidecadal timescales. Nature 499:464–467

Haarsma R, Hazeleger JW (2007) Extratropical atmospheric response to equatorial Atlantic cold tongue anomalies. J Clim 20:2076–2091

Häkkinen S, Rhines PB, Worthen DL (2011) Atmospheric blocking and Atlantic multidecadal ocean variability. Science 334:655–659

Hodson DLR, Sutton RT, Cassou C, Keenlyside N, Okumura Y, Zhou TJ (2010) Climate impacts of recent multidecadal changes in atlantic ocean sea surface temperature: a multimodel comparison. Clim Dyn 34:1041–1058

Honda M, Inoue J, Yamane S (2009) Influence of low Arctic sea ice minima on anomalously cold Eurasian winters. Geophys Res Lett 36:L08707. doi:10.1029/2008GL037079

Hoskins BJ, Karoly DJ (1981) The steady linear response of a spherical atmosphere to thermal and orographic forcing. J Atmos Sci 38:1179–1196. doi:10.1175/1520-0469(1981)038<1179:TSLROA>2.0.CO;2

Hoskins BJ, James IN, White GH (1983) The shape, propagation and mean-flow interaction of large-scale weather systems. J Atmos Sci 40:1595–1612

Hurrell J, van Loon WH (1997) Decadal variations in climate associated with the North Atlantic Oscillation. Clim Change 36:301–326

Jungclaus JH, Haak H, Latif M, Mikolajewicz U (2005) Arctic-North Atlantic interactions and multidecadal variability of the meridional overturning circulation. J Clim 18:4013–4031

Kavvada A, Ruiz-Barradas A, Nigam S (2013) AMO's structure and climate footprint in observations and IPCC AR5 climate simulations. Clim Dyn. doi:10.1007/s00382-013-1712-1

Keenlyside NS, Omrani N-E (2014) Has a warm North Atlantic contributed to recent European cold winters? Environ Res Lett 9:061001

Kerr RA (2000) A North Atlantic climate pacemaker for the centuries. Science 288(5473):1984–1986

Knight JR, Folland CK, Scaife AA (2006) Climate impacts of the Atlantic Multidecadal Oscillation. Geophys Res Lett 33:L17706. doi:10.1029/2006GL026242

Knudsen MF, Seidenkrantz MS, Jacobsen BH, Kuijpers A (2011) Tracking the Atlantic Multidecadal Oscillation through the last 8000 years. Nat Commun 2:1–8

Knudsen MF, Jacobsen BH, Seidenkrantz M-S, Olsen J (2014) Evidence for external forcing of the Atlantic Multidecadal Oscillation since termination of the Little Ice Age. Nat Commun 5:3323. doi:10.1038/ncomms4323

Kuhlbrodt T, Griesel A, Montoya M, Levermann A, Hofmann M, Rahmstorf S (2007) On the driving processes of the Atlantic meridional overturning circulation. Rev Geophys 45:RG2001. doi:10.1029/2004RG000166

Kushnir Y, Robinson WA, Bladé I, Hall NMJ, Peng S, Sutton R (2002) Atmospheric GCM response to extratropical SST anomalies: synthesis and evaluation. J Clim 15:2233–2256

Kwon Y-O, Deser C, Cassou C (2011) Coupled atmosphere-mixed layer ocean response to ocean heat flux convergence along the Kuroshio Current Extension. Clim Dyn. doi:10.1007/s00382-010-0764-8

Liu J, Curry JA, Wang H, Song M, Horton RM (2012) Impact of declining Arctic sea ice on winter snowfall. Proc Natl Acad Sci USA. doi:10.1073/pnas.1118734109

Magnusdottir G, Deser C, Saravanan R (2004) The effects of North Atlantic SST and sea ice anomalies on the winter circulation in CCM3, Part I: Main features and storm-track characteristics of the response. J Clim 17:857–876

Medhaug I, Furevik T (2011) North Atlantic 20th century multidecadal variability in coupled climate models: sea surface temperature and ocean overturning circulation. Ocean Sci 7:389–404

Msadek R, Frankignoul C, Li L (2011) Mechanisms of the atmospheric response to North Atlantic multidecadal variability: a model study. Clim Dyn 36:1255–1276

Neale RB et al (2011) Description of the NCAR Community Atmosphere Model (CAM5). National Center for Atmospheric Research Tech. Rep. NCAR/TN-486+STR

Okumura Y, Xie SP, Numaguti A, Tanimoto Y (2001) Tropical Atlantic air–sea interaction and its influence on the NAO. Geophys Res Lett 28:1507–1510

Okumura YM, Deser C, Hu A, Timmermann A, Xie S-P (2009) North Pacific climate response to freshwater forcing in the subarctic North Atlantic: oceanic and atmospheric pathways. J Clim 22:1424–1445

Omrani NE, Keenlyside NS, Bader JR, Manzini E (2014) Stratosphere key for wintertime atmospheric response to warm Atlantic decadal conditions. Clim Dyn 42:649–663

Omrani NE, Bader J, Keenlyside NS, Manzini E (2015) Troposphere–stratosphere response to large-scale North Atlantic Ocean variability in an atmosphere/ocean coupled model. Clim Dyn. doi:10.1007/s00382-015-2654-6

Otterå OH, Bentsen M, Drange H, Suo L (2010) External forcing as a metronome for Atlantic multidecadal variability. Nat Geosci 3:688–694

Park S, Deser C, Alexander MA (2005) Estimation of the surface heat flux response to sea surface temperature anomalies over the global oceans. J Clim 18:4582–4599

Peings Y, Magnusdottir G (2014a) Forcing of the wintertime atmospheric circulation by the multidecadal fluctuations of the North Atlantic ocean. Environ Res Lett 9(3):034018

Peings Y, Magnusdottir G (2014b) Response of the wintertime Northern Hemisphere atmospheric circulation to current and projected Arctic sea ice decline: a numerical study with CAM5. J Clim 27:244–264

Peings Y, Magnusdottir G (2015) The role of sea surface temperature, Arctic sea ice and Siberian snow in forcing the atmospheric circulation in winter of 2012–2013. Clim Dyn. doi:10.1007/s00382-014-2368-1

Peings Y, Saint-Martin D, Douville H (2012) A numerical sensitivity study of the Siberian snow influence on the northern annular mode. J Clim 25:592–607

Peng S, Whitaker JS (1999) Mechanisms determining the atmospheric response to midlatitude SST anomalies. J Clim 12:1393–1408

Peng S, Robinson WA, Li S, Hoerling MP (2005) Tropical Atlantic SST forcing of coupled North Atlantic seasonal responses. J Clim 18:480–496. doi:10.1175/JCLI-3270.1

Rayner NA, Parker DE, Horton EB, Folland CK, Alexander LV, Rowell DP, Kent EC, Kaplan A (2003) Global analyses of sea surface temperature, sea ice, and night marine air temperature since the late nineteenth century. J Geophys Res 108(14):4407. doi:10.1029/2002JD002670

Richter JH, Sassi F, Garcia RR (2010) Toward a physically based gravity wave source parameterization in a general circulation model. J Atmos Sci 67(1):136–156. doi:10.1175/2009JAS3112.1

Ruprich-Robert Y, Cassou C (2014) Combined influences of seasonal East Atlantic Pattern and North Atlantic Oscillation to excite Atlantic multidecadal variability in a climate model. Clim Dyn. doi:10.1007/s00382-014-2176-7

Sato K, Inoue J, Watanabe M (2014) Influence of the Gulf Stream on the Barents Sea ice retreat and Eurasian coldness during early winter. Environ Res Lett 9:084009

Schlesinger ME, Ramankutty N (1994) An oscillation in the global climate system of period 65–70 years. Nature 367:723–726

Smith KL, Neely RR, Marsh DR, Polvani LM (2014) The specified chemistry whole atmosphere community climate model (SC-WACCM). J Adv Model Earth Syst 6:883–901. doi:10.1002/2014MS000346

Sutton RT, Hodson DLR (2005) Atlantic Ocean forcing of North American and European summer climate. Science 309:115–118

Sutton RT, Hodson DLR (2007) Climate response to basin-scale warming and cooling of the North Atlantic Ocean. J Clim 20:891–907. doi:10.1175/JCLI4038.1

Sutton R, Mathieu PP (2002) Response of the atmosphere–ocean mixed layer system to anomalous ocean heat flux convergence. Q J R Meteorol Soc 128:1259–1275

Terray L, Cassou C (2002) Tropical Atlantic sea surface temperature forcing of quasi-decadal climate variability over the North Atlantic-European region. J Clim 15:3170–3187

Timmermann A, Latif M, Voss R, Grötzner A (1998) Northern Hemisphere interdecadal variability: a coupled air–sea mode. J Clim 11:1906–1931

Ting M, Kushnir Y, Seager R, Li C (2011) Robust features of Atlantic multi-decadal variability and its climate impacts. Geophys Res Lett 38:L17705. doi:10.1029/2011GL048712

Vihma T (2014) Effects of Arctic sea ice decline on weather and climate: a review. Surv Geophys. doi:10.1007/s10712-014-9284-0

Wallace JM, Held IM, Thompson DWJ, Trenberth KE, Walsh JE (2014) Global warming and winter weather. Science 343(6172):729–730. doi:10.1126/science.343.6172.729

Walsh JE, Chapman WL (2001) 20th-century sea–ice variations from observational data. Ann Glaciol 33:444–448

Wang C, Zhang L (2013) Multidecadal ocean temperature and salinity variability in the tropical North Atlantic: linking with the AMO, AMOC, and subtropical cell. J Clim 26:6137–6162. doi:10.1175/JCLI-D-12-00721.1

Wang C, Xie S-P, Carton JA (2004) A global survey of ocean–atmosphere interaction and climate variability. In: Wang C, Xie SP, Carton JA (eds) Earth's climate. American Geophysical Union, Washington, D.C. doi:10.1029/147GM01

Wang C, Dong S, Evan AT, Foltz GR, Lee S-K (2012) Multidecadal covariability of North Atlantic sea surface temperature, African dust, Sahel rainfall, and Atlantic hurricanes. J Clim 25:5404–5415

Watson PAG, Gray LJ (2014) How does the quasi-biennial oscillation affect the stratospheric polar vortex? J Atmos Sci 71:391–409. doi:10.1175/JAS-D-13-096.1

Xie S-P, Carton JA (2004) Tropical Atlantic variability: patterns, mechanisms, and impacts. In: Wang C, Xie SP, Carton JA (eds) Earth climate: the ocean-atmosphere interaction. Geophysical monograph series 147. AGU, Washington, pp 121–142

Zhang R, Delworth TL (2006) Impact of Atlantic multidecadal oscillations on India/Sahel rainfall and Atlantic hurricanes. Geophys Res Lett. doi:10.1029/2006GL026267

Zhang L, Wang C (2013) Multidecadal North Atlantic sea surface temperature and Atlantic meridional overturning circulation variability in CMIP5 historical simulation. J Geophys Res Oceans 118:5772–5791. doi:10.1002/jgrc.20390